Department of Electrical
and
Computer Systems Engineering

Technical Report
MECSE-12-2003

A mechanism to facilitate the building of structures with robotic swarms

Robert L. Stewart and R. Andrew Russell

MONASH
UNIVERSITY

A mechanism to facilitate the building of structures with robotic swarms

Robert L. Stewart and R. Andrew Russell

Intelligent Robotics Research Centre,
Monash University, Clayton, VIC 3800, Australia.
{Robert.Stewart, Andy.Russell}@eng.monash.edu.au

Abstract. In this report progress towards the development of a mechanism that will facilitate the building of structures by a robotic swarm is detailed. While the results recorded are preliminary and represent work in progress, it has been found that the implementation method for the conceived idea of utilising a light-field template that varies in both space and time is valid.

1 Introduction

This report details progress towards the development of a mechanism that will facilitate the building of structures by a robotic swarm. The work builds on previous research [1] inspired by social insects. In that work it was found that a light source can cause a light-field template to be established in the environment and that robots, like insects, can utilise such a template to guide their building activities.

We are interested in mounting light sources on robots to investigate cooperative building behaviours. We require a robust light source detection mechanism and it is towards this goal that the research outlined in this report is directed.

2 Transmitter mechanism

The transmitter mechanism consists of two beams of light pulsed at 500Hz. The intensity of each beam is capable of being varied. A beacon that effectively pulses at 50Hz emits light from the transmitter in all other directions. The system is conveniently represented as shown in Figure 1.

A prototype transmitter has been implemented (Figure 2). LEDS 1 and 2 are pulsed at 500Hz and the motor, with a mirror attached at 45˚, runs at 3000rpm (50Hz) shining the light from LED 3 in all directions of the horizontal plane.

The electronic circuit that was designed to drive the transmitter is shown in Figure 3. The intensity of 500Hz light can be readily changed by varying the current through

each led. This can be done by varying V_{con}. By connecting V_{con}, via a voltage buffer, to a microcontroller's DAC (Digital to Analogue Converter), the intensity of light can be controlled automatically.

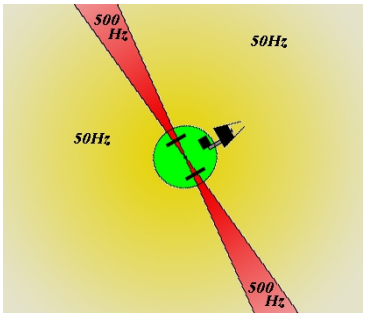

Fig. 1. Graphical representation of a robot equipped with a transmitter. The intensity of the two 500Hz beams (shown in red) decreases with the distance from the robot. Similarly, the intensity of the 50Hz beacon source (shown in yellow) also decreases with distance

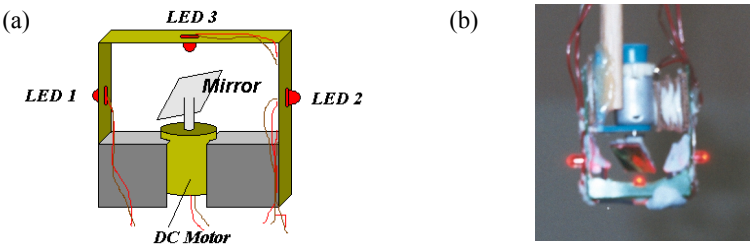

Fig. 2. Illustration, (a), and photo, (b), of a prototype transmitter. A mirror is attached to the motor shaft at approximately 45˚ to the horizontal

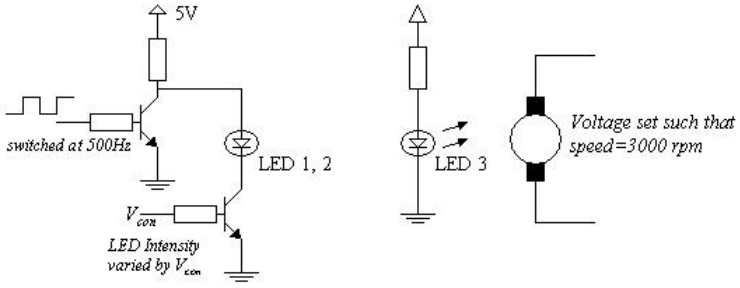

Fig. 3. General circuit design used to drive the transmitter

3 Receiver

In order for a robot to be able to detect the 50Hz beacon and 500Hz beams quickly, a sensor ring has been developed (see Figure 4). The sensor ring consists of 24 phototransistors each with approximately 15˚ acceptance angle. When arranged in a ring, 360˚ of coverage is obtained. Note, there will be some overlap in the coverage each sensor provides.

(a) (b)

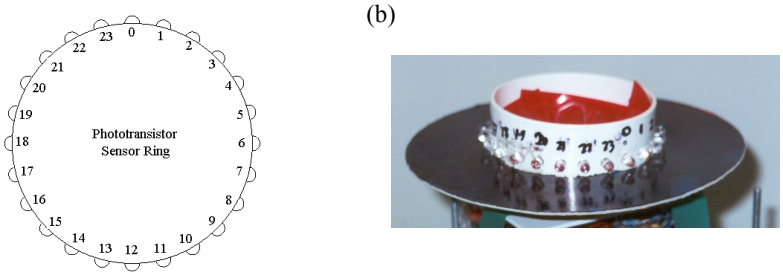

Fig. 4. (a) Sensor ring with 24 equally spaced phototransistors. (b) Prototype sensor ring.

4 Detection scheme

We require a means of determining the intensity of 50Hz and 500Hz light incident on each phototransistor in the sensor ring in the presence of noise. In an indoor environment there are likely to be fluorescent lights in use. A typical photodetector response to these lights is shown below (Figure 5):

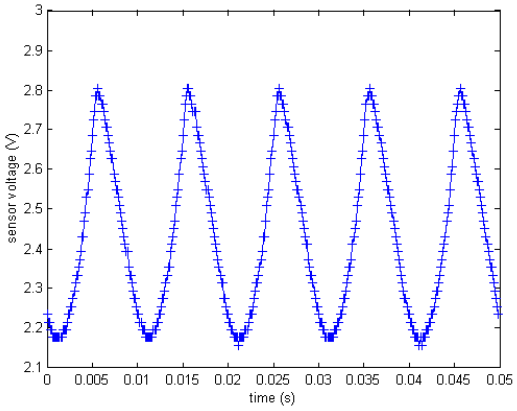

Fig. 5. A typical sensor response to the fluorescent lights indoors. The sample rate was 8000Hz

We have modeled this noise source as a rectified sinusoidal waveform at 100Hz reflected over the x-axis. A Fourier series representation is (without scaling):

$$f_{100}(t) = -\frac{2}{\pi} + \sum_{n=1}^{\infty} \frac{4\pi}{\pi^2 - 4n^2\pi^2} \sin\left(\frac{\pi}{2} - n\pi\right) \cos(n \cdot 2\pi 100t) \tag{1}$$

The signal from each photodetector is assumed to be periodic. Thus, it can be represented as follows (here [2, 3] have been used):

$$f(t) = A\sin(2\pi 50t + \varphi_1) + B\sin(2\pi 500t + \varphi_2) + a_0 + \sum_{n=1}^{\infty} \left(a_n \sin(2\pi f_n t) + b_n \cos(2\pi f_n t)\right) \tag{2}$$

Here the first two terms represent the fundamental frequencies from the 50Hz and 500Hz periodic sources (generated by the transmitter). The infinite sum represents the higher order harmonics from the 50Hz and 500Hz sources as well as all noise sources such as those generated by the fluorescent lights.

The detected intensities of the 50Hz and 500Hz sources are related to the magnitude of A and B, in (2), respectively. By bandpass filtering the signal, (2), to remove the extraneous components and then calculating the RMS (Root Mean Square) value of the resulting waveform, approximations to A and B can then be made. Ideally we would have two filters such that the output of each would be a pure sinusoidal waveform. That is,

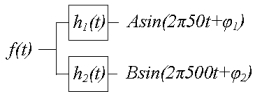

Fig. 6. Ideal filters that extract the desired components from *f(t)*

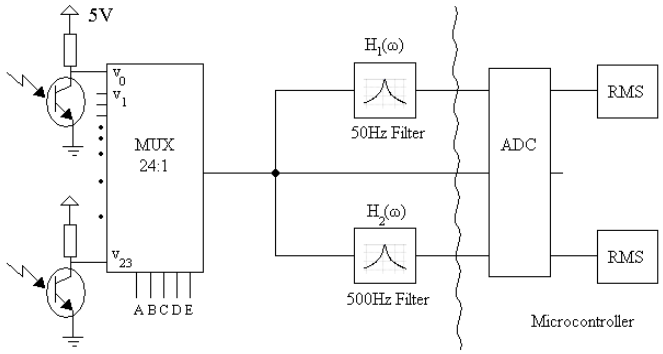

Fig. 7. The complete detection system

To reduce the duplication of circuitry (by having two filters for each detector), an analogue multiplexor was used to steer the signal from the selected detector (within the sensor ring) to the two analogue filters. The complete system diagram is shown in Figure 7.

The following graphs (Figures 8 and 9) show typical responses when detecting the 50Hz beacon and the 500Hz beacon. The results shown in Figure 8 were obtained with the fluorescent lights switched off. For the results shown in Figure 9, the lights were switched on resulting in a noisy signal.

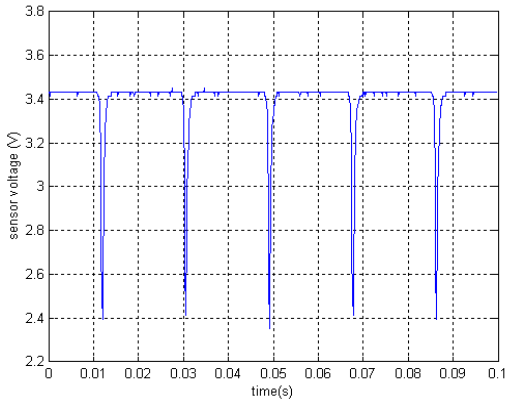

Fig. 8. A typical response when detecting the 50Hz beacon source. The light is only incident on the phototransistor for a short period of time in each cycle. This results in a spike. Note that a small voltage indicates high intensity light

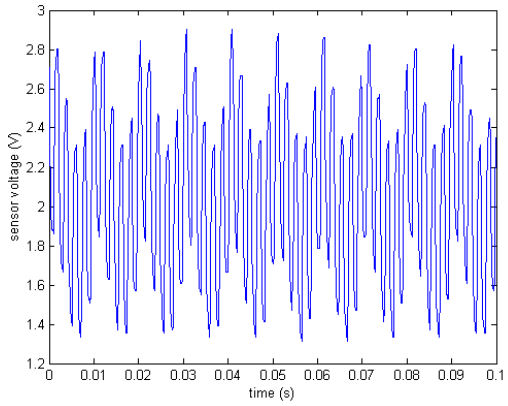

Fig. 9. A typical response from a detector in the presence of the 500Hz source as well as 100Hz noise resulting from the fluorescent lights (similar to that in Figure 5)

The response shown in Figure 8 has been modeled with the following equation:

$$y_{out}(t) = \sum_{n=0}^{\infty} \frac{4(b-a)L}{dn^2\pi^2}\left(\cos\left(\frac{n\pi d}{2L}\right)-1\right)\cdot\cos\left(\frac{n\pi t}{L}\right) \quad \textbf{(3)}$$

where the parameters a, b, d and L define the properties of the waveform as shown below (Figure 10):

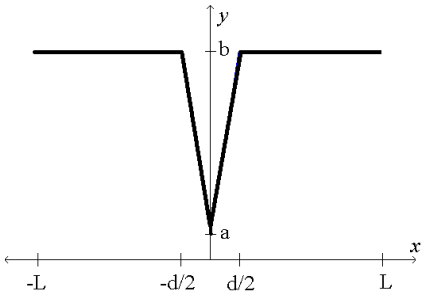

Fig. 10. Parameter definitions for equation 3

Using (3), the response shown in Figure 8 can be modeled (see Figure11).

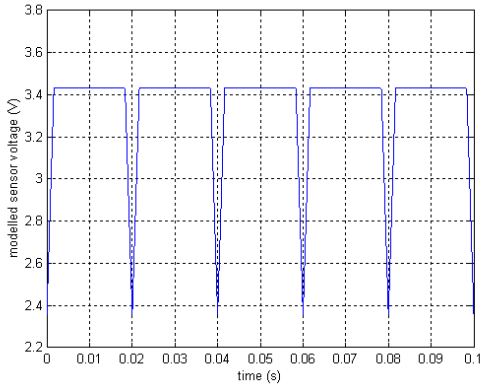

Fig. 11. A model of the response shown in Figure 8. Here d=L/3=0.01/3. Note also that the phase delay has been neglected

Figure 12 shows the power spectrum for three different values of *d*. For a small value of *d*/*L*=1/3 the power is spread somewhat more evenly amongst the harmonic components than when *d*/*L* is close to unity. In this latter case, most of the energy is confined to the first two harmonics. Figure 8 reveals that the actual response typically is closest to *d*/*L*=1/3 which, based on Figure 12, means that we have a feasible chance of detecting any of the first five (say) harmonics.

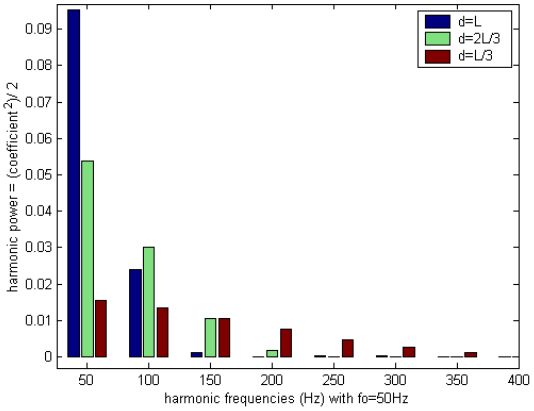

Fig. 12. Harmonic power spectrum of the first seven harmonics showing the distribution of power for different values of *d*

5 Filter design

As shown in Figures 6 and 7, two bandpass filters are required to extract the 50Hz and 500Hz sinusoidal components of the detected signal. A state-variable filter implementation was chosen (see [4, 5] for details). The transfer function of which is given by:

$$T(s) = \frac{V_{out}(s)}{V_{in}(s)} = \frac{as}{s^2 + s\frac{\omega_0}{Q} + \omega_0^2} \tag{4}$$

Since each sensor in the sensor ring will be using the same filter circuit, a settling time must be waited after switching the signal through using the multiplexor. The bandpass filter is centred on the frequency we are trying to detect, namely $\omega_0=2\pi f_0$. If the filter is subjected to a sinusoidal input of that frequency such as:

$$v_{in}(t) = u(t)\sin\omega_0 t \tag{5}$$

the output can be evaluated using inverse Laplace transform techniques and is of the form [2]:

$$v_{out}(t) = e^{-\sigma t}\left(A\cos\omega_d t + \frac{B-\sigma A}{\omega_d}\sin\omega_d t\right) + C\cos\omega_0 t + \frac{D}{\omega_0}\sin\omega_0 t \tag{6}$$

Before the signal can be sampled by the ADC, time must be waited for the transient component to decay. The settling time is taken to be five time constants and is given by:

$$\text{settling time} = 5\tau = \frac{5}{\sigma} = \frac{10Q}{\omega_0} \tag{7}$$

As can be seen from (7), the settling time is dependent on the filter's Q value and ω_0, the frequency we are trying to detect. The time for a full sensing cycle (involving all 24 photodetectors) can be calculated by the following equation:

$$\text{Total sensing cycle time} = 24 \times (\text{settling time} + (\text{number of samples} \times \text{sampling rate})) \tag{8}$$

A bandpass filter centred about $\omega_0=2\pi50$ was designed and implemented using single-supply operational amplifiers. An input voltage buffer stage as well as an output gain stage were also used in the circuit (see Figure 13).

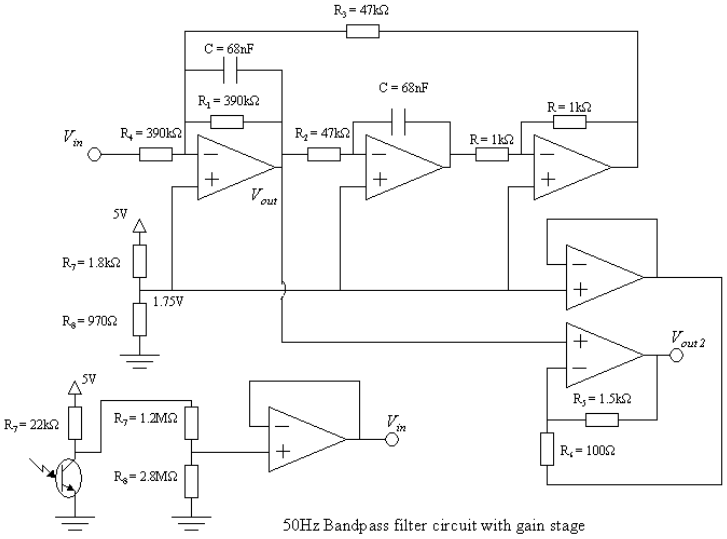

Fig. 13. Bandpass filter (Q=8.3, $\omega_0=2\pi50$) with additional input and output stages

In terms of component values, the bandpass filter equation of (4) is given by:

$$T(s) = \frac{V_{out}(s)}{V_{in}(s)} = \frac{\frac{1}{R_4 C}s}{s^2 + \frac{1}{R_1 C}s + \frac{1}{(R_2 C)^2}} \tag{9}$$

For the design in Figure 13, Q=8.3 and $\omega_0=2\pi50$. Using these values and (7), the total settling time can be calculated and is equal to 6.34s. This value is too high for real-time operation. To remedy this situation, another filter with a faster settling time could be sought or the filter could be redesigned to detect a higher order harmonic. This is a feasible alternative, since as Figure 12 reveals, much of the harmonic energy is not confined to the fundamental frequency (50Hz). If for example $\omega_0=2\pi250$, the

settling time could be reduced by a factor of 5 giving 1.27s. In addition to this, the speed of the motor could also be increased somewhat. This would increase the fundamental frequency further reducing the settling time.

A Bode plot of the filter circuit (Figure 13) is shown below (Figure 14).

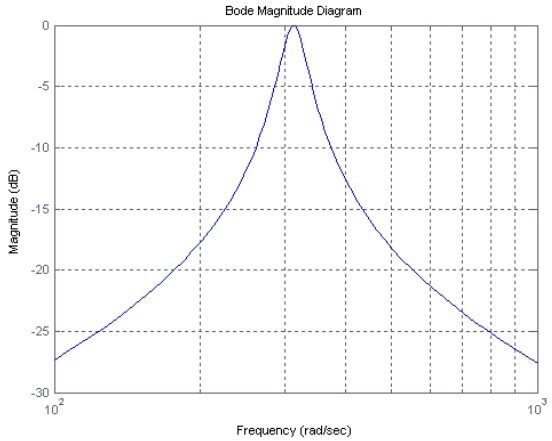

Fig. 14. Bode plot of the filter circuit shown in Figure 13

A second bandpass filter (Q=25, ω_0=2π500) was designed and implemented. As Figure 9 reveals, the 500Hz input signal was more sinusoidal (neglecting noise) in appearance than the signal generated from the beacon (Figure 8). This meant much of the harmonic energy was confined to the fundamental harmonic and as such a gain stage did not appear to be required. For future designs however, a gain stage will be added in order to utilise the maximum swing range of the op-amps. This will result in the use of more quantisation levels when the output signal is sampled by the microcontroller's ADC.

Again, a long settling time (=1.91s) is an issue that needs resolving. In this case however, the solution is somewhat easier. Either ω_0 can be readily increased (on the transmitter and receiver ends) or Q can be decreased.

6 Results obtained from filtering

With the filters implemented it was possible to test the system. When the beacon signal shown in Figure 8 was obtained, it was also filtered and sampled. Figures 15 and 16 show the filtered response (after the minimum settling time has been waited) from the 50Hz bandpass filter and the 500Hz bandpass filter. As can be seen in Figure 15, the fundamental frequency component expected in (3) is present. In Figure 16 however, the signal is minimal, as required, possibly with a contribution from the

beacon source (10^{th} harmonic). When the 100Hz noise signal is present we would also expect to see a component from the 100Hz (5^{th} harmonic) noise source. Also, since the filters are not ideal (as assumed in Figure 6), we could expect other frequency components to pass through the filter (albeit greatly attenuated by the filter).

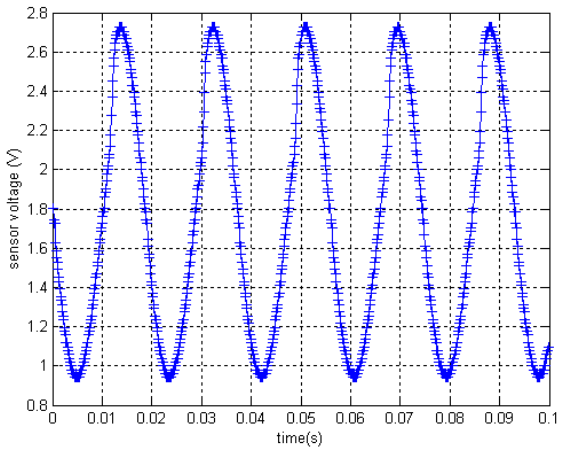

Fig. 15. The response obtained when the signal shown in Figure 8 was filtered by the 50Hz bandpass filter. The fundamental 50Hz harmonic component has been clearly extracted. Note that the 100Hz noise source was not present in this example

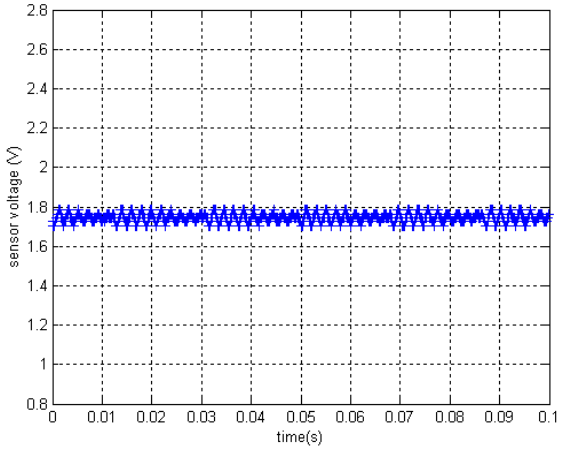

Fig. 16. The response obtained when the signal shown in Figure 8 was filtered by the 500Hz bandpass filter. Only a small component, possibly a contribution from the 10^{th} harmonic of the beacon source, is evident

A similar situation is evident when the 500Hz beam is incident on a detector. The response shown earlier in Figure 9 is a typical signal with 100Hz noise clearly evident. When filtered by the 500Hz bandpass filter the 500Hz fundamental harmonic passes through the filter (see Figure 17). Note that the 100Hz noise has been sufficiently attenuated by the filter, as desired. Figure 18 shows the response at the output of the 50Hz bandpass filter. While there is no 50Hz component present, unfortunately a signal is still registered since the 100Hz noise has passed through the filter, albeit attenuated. It is hoped that this will not be such a problem in future implementations when a higher order harmonic is to be detected.

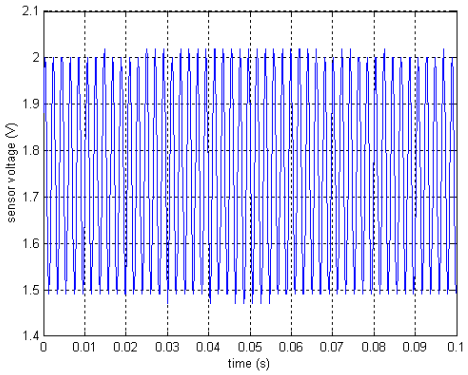

Fig. 17. The result of filtering the signal shown in Figure 9 with a 500Hz bandpass filter

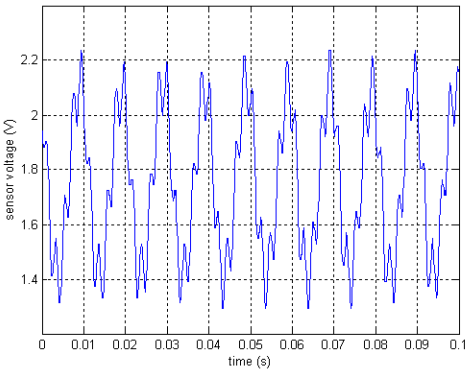

Fig. 18. The result of filtering the signal in Figure 9 with a 50Hz bandpass filter. Despite the fact that the detector has not been exposed to a 50Hz signal, a result is still recorded due to 100Hz noise passing through the filter (albeit attenuated)

7 Interpreting the signals

As the receiver circuit shown in Figure 7 illustrates, once the detected signal has been filtered it is sampled by the ADC of a microcontroller. Typical results obtained from this process were shown in Section 6. To quantitatively determine the relative magnitude of the filtered signals, the Root Mean Square (RMS) values are calculated. The formula used is [6] :

$$RMS = \sqrt{\frac{\sum_{n=0}^{N} y_n^2}{N}} \qquad (10)$$

where N is the number of samples and y_n is a sample (with the 1.75V bias removed)

After each sensing cycle the following data arrays have been filled:

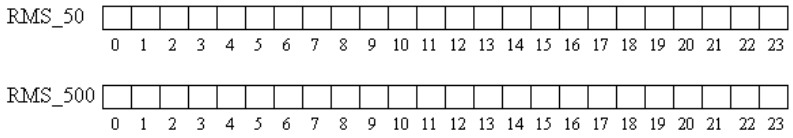

Fig. 19. After each sensing cycle two data arrays have been filled. They contain the RMS values calculated for each detector in the sensor ring

The first array, RMS_50, contains the RMS values of the 50Hz bandpass filtered responses (one value for each detector) and similarly, the second array, RMS_500, contains the values of the 500Hz bandpass filtered responses. Note that since single supply op-amps were used, the filtered responses have an offset of approximately 1.75V. Before calculating the RMS value of each signal, this bias was first subtracted.

Some initial tests were carried out to see if the intensity of the detected signal increases as the robot approaches the light source. Figure 20 shows two responses obtained (from detector number 0) when the robot was driven directly towards the beacon source. One response is with the fluorescent lights on and the second is with them off. As was hoped, the RMS value obtained increases as the robot approaches the light source. However, a similar problem to that discussed in Section 6 is evident. When the 50Hz light intensity is low, the 100Hz noise can corrupt the signal. It is hoped that by detecting a higher order harmonic this problem will not be as significant.

Similar results are obtained when the robot drives along a 500Hz beam towards the light source (in the presence of 100Hz noise). Figure 21 shows a family of curves obtained for four different source light intensities. By increasing the source light intensity at the transmitter end, the response at the detector end can be made to shift towards the right. This feature will prove to be useful in the future.

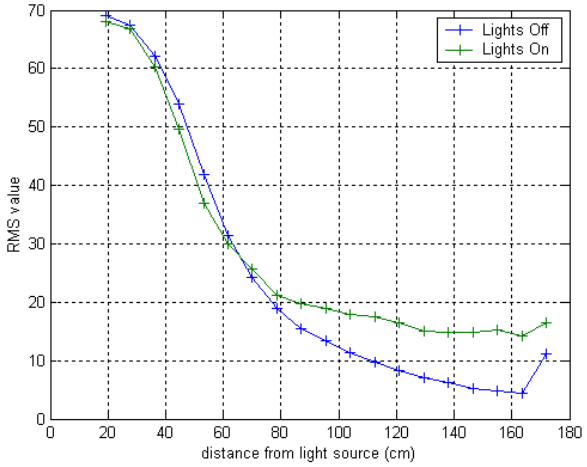

Fig. 20. Responses obtained from sensor number 0 when the robot drives towards the beacon source with and without the presence of 100Hz noise

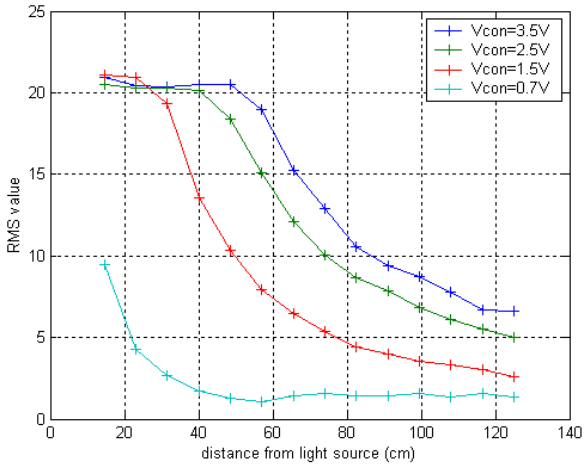

Fig. 21. Family of curves obtained when the robot drives along a 500Hz beam produced by the transmitter. By increasing the source intensity (increasing V_{con}) the response can be made to shift towards the right

8 Obtaining a picture of the environment

In the previous experiments RMS values of the filtered signals were calculated for just one sensor (the one facing the direction of travel). However, there are 23 detectors in the sensor ring. For each sensing cycle the arrays in Figure 19 are filled with data. It is interesting to see how the values in this array change as the robot moves through its environment.

The path shown in Figure 22 was chosen for the robot. It consists of 20 stops at which a sensing cycle was performed.

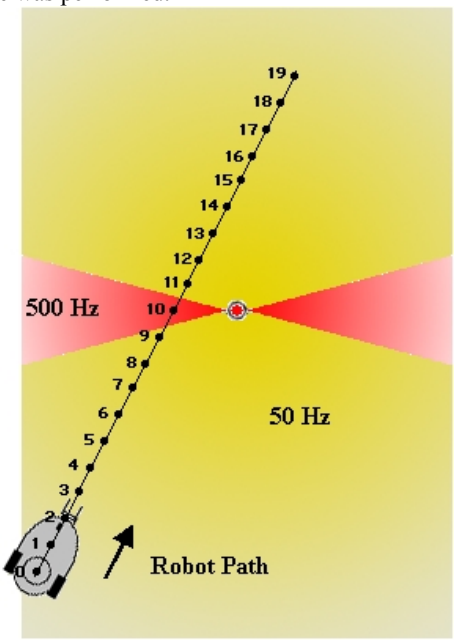

Fig. 22. Graphical depiction of the chosen path taken by the robot. Initially it starts in a region where only the 50Hz beacon is visible. Approximately midway through it's journey it moves across one of the 500Hz beams produced by the transmitter. The closer the robot is to the source, the higher the expected RMS value we would expect to obtain. The red and yellow shading has been used for illustration purposes only

As the robot moved along its path the light became incident on different detectors with a strength dependent on the distance from the source. The information is depicted in Figures 23 and 24. In Figure 23 it can seen that there is a gap in plot. That is, the 50Hz signals obtained from each sensor in the sensor ring were low around step 10. From Figure 22 it can be seen that it is at this point that the robot is crossing out of the 50Hz light into the 500Hz beam. As such, there is a large signal evident in Figure 24 around step 10. Figures 25 and 26 depict this situation more readily.

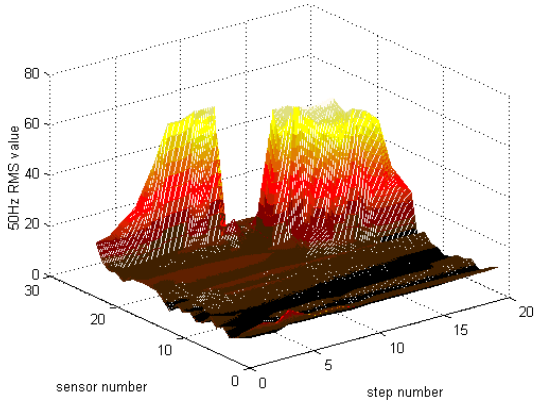

Fig. 23. Plot showing how the 50Hz signal strength varies for each detector in the sensor ring as the robot moved along the path shown in Figure 22

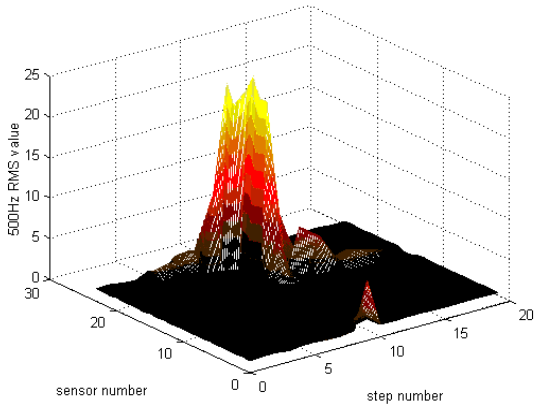

Fig. 24. Plot showing how the 500Hz signal strength varies for each detector in the sensor ring as the robot moved along the path shown in Figure 22

It is interesting to note that in Figure 26 there is a "shadow" of the results displayed in Figure 25. That is, the 10^{th} harmonic of the 50Hz source is passing through the 500Hz bandpass filter and registering a result.

As the results show, the sensor ring is able to determine the direction of the two light sources simultaneously (for practical purposes) as well as obtaining light intensity (function of distance) information.

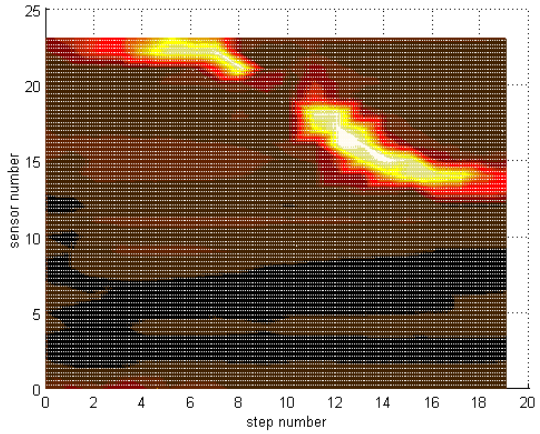

Fig. 25. Alternative representation of the plot shown in Figure 23. A gap can be seen around step 10 when the robot moves out of the 50Hz light into the 500Hz beam

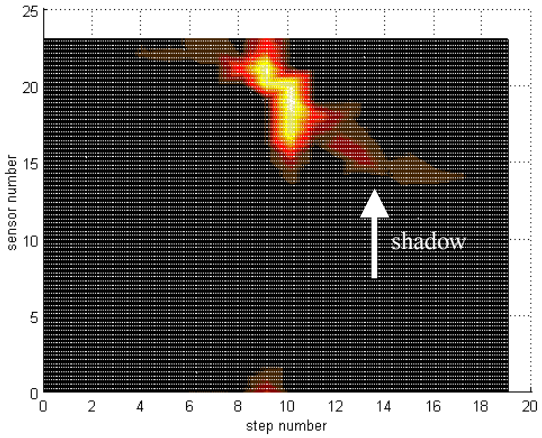

Fig. 26. Alternative representation of the plot shown in Figure 24. Around step 10 the robot moves into the 500Hz beam. As such the signal is strong here. A "shadow" of the result shown in Figure 25 is also evident

9 Conclusion

The results presented in this report document work in progress. The results and descriptions given are a first attempt to present and discuss some of the work currently being undertaken for a postgraduate thesis project on *Building structures with robotic swarms*. Undoubtedly some of the statements made and terms used will be erroneous and require correction.

The report details a mechanism that will facilitate the building of structures with robotic swarms. The trials have confirmed the validity of our conceived implementation method for spatiotemporal varying templates. A transmitter and receiver have been documented as well as a detection scheme that is capable of quantitatively measuring the intensity of 50Hz and 500Hz light incident on a sensor ring.

Researchers interested in building beacons for localisation may find some use in this work. A cheap transmitter (built with a motor, mirror and LED) can radiate light in all directions. Provided the filtering is robust to 100Hz noise, range data can be obtained by using the intensity of light which was shown to decrease as distance from the beacon was increased.

Future work will look at ways of increasing the sensing cycle time as well as making the system more robust to the 100Hz noise created by fluorescent lights.

Acknowledgements

This project is supported by a grant from Monash University's Faculty of Engineering Small Grants Scheme. Robert Stewart would like to acknowledge the support of an Australian Postgraduate Award. The help and advice of academic and support staff within the Department of ECSE, Monash University, has been appreciated.

References

[1] R. Stewart and R. A. Russell, "Emergent structures built by a minimalist autonomous robot using a swarm-inspired template mechanism," presented at First Australian Conference on Artifical Life (ACAL), Canberra, 2003.

[2] E. Kreyszig, *Advanced engineering mathematics*, 8th ed. New York: John Wiley, 1998.

[3] C. D. McGillem and G. R. Cooper, *Continuous and discrete signal and system analysis*, 3rd ed. Philadelphia: Saunders College Pub., 1991.

[4] A. B. Williams, *Active Filter Design*, 1975.

[5] M. G. Ellis, *Electronic filter analysis and synthesis*. Boston: Artech House, 1994.

[6] H. Kwakernaak, R. Sivan, and R. C. W. Strijbos, *Modern signals and systems*. Englewood Cliffs, N.J.: Prentice Hall, 1991.